

Physical Characterisation of Electrospun PVDF/PVA Nanofibre Membrane as a Potential Artificial Soft Tissue Scaffold Application

Mohd Syahir Anwar Hamzah¹, Celine Ng¹, Ashari Kasmin¹, Latifah Md Ariffin², Saiful Izwan Abd Razak³ and Nadirul Hasraf Mat Nayan^{4*}

¹Faculty of Engineering Technology, Universiti Tun Hussein Onn Malaysia, Pagoh Higher Education Hub, Jalan Panchor, Pagoh, Johor, 84600, Malaysia.

²Faculty of Mechanical Engineering and Manufacturing, Universiti Tun Hussein Onn Malaysia, Parit Raja, Johor, 84600, Malaysia.

³Centre of Advanced Composite, Faculty of Engineering, Universiti Teknologi Malaysia, Jalan Universiti, Skudai, Johor, 81310, Malaysia.

⁴Microelectronics and Nanotechnology-Shamsuddin Research Centre, Universiti Tun Hussein Onn Malaysia, Parit Raja, Johor, 86400, Malaysia.

Received 19 June 2020, Accepted 20 September 2020

ABSTRACT

The application of nanofibrous scaffold in tissue engineering has great potential in solving the drawbacks of conventional tissue/organ transplant procedures. This present work aims to evaluate the effect of polyvinyl alcohol (PVA) inclusion on the physical properties of polyvinylidene fluoride (PVDF) nanofibrous membrane fabricated via the electrospinning method and its potential as an artificial tissue scaffold. The physical performance of electrospun PVDF/PVA samples was assessed by field emission scanning electron microscope (FESEM), tensile strength, water contact angle (WCA), degree of swelling, conductivity level, and Fourier transform infrared (FTIR) spectroscopy. Based on the physical characterisations, sample 90PVDF/10PVA with the PVDF-to-PVA ratio of 90:10 was the optimum composition, where the electrospun samples exhibit the most balanced properties that meet the requirement for artificial soft tissue replacement. In vitro studies using human dermal fibroblast (HDF) cells show that the PVDF/PVA nanofibrous scaffold successfully enhanced the adhesion and proliferation of cells compared to the neat PVDF scaffold as indicated by the MTT assay and Live/Dead kit. Overall results show the potential of PVDF/PVA nanofibrous membrane as a promising material suitable for soft tissue engineering applications.

Keywords: Polyvinylidene Fluoride, Polyvinyl Alcohol, Electrospinning, Tissue Engineering, Nanofibre Scaffold.

1. INTRODUCTION

In tissue engineering, nanofibre-based scaffold is favourable for nerve, skin, cartilage, and other soft tissue replacement applications. The tissue scaffold provides a provisional matrix to facilitate the regeneration of damaged tissues by remodelling tissue functions and supporting cell growth throughout the artificial microarchitecture [1-3]. For clinical applications, the mechanical properties of tissue scaffold should be sufficient to withstand internal and external forces depending on the types of tissue and organ. Besides, the tissue scaffold must be biocompatible with good hydrophilic characteristic and high surface area-to-volume ratio to expedite cell seeding and the diffusion of nutrients through the artificial tissue structure [3].

*Corresponding Author: nadirul@uthm.edu.my

Electrospinning is a simple technique that has been widely used due to its ability to fabricate with controllable surface morphology, versatile porosity, and optimal mechanical performance, which is favourable for preparing nanofibre scaffold. Studies show that the alignment and diameter of fibres tailored using electrospinning can be tuned to meet the specific design of wide range of cells / tissues which highly influences the cell growth, degradation rates, physical

condition, and mechanical properties of artificial scaffold [4-5]. Therefore, the selection of materials is crucial because the success of electrospinning process depends on the ability of polymer solution in forming a fine charged jet when a strong electric field is applied.

Polyvinylidene fluoride (PVDF) is a semi-crystalline polymer structure and could exist in different possible polymorphism phases which are α , β , γ , and δ [6]. Previous study on the electrospinning of PVDF shows that the dominant orientation crystalline structure of polar β -phase crystal along the fibre axis, which gives high electric conductivity behaviour, makes it suitable for tissue engineering [7]. The major drawback of PVDF in tissue engineering is that it is not a hydrophilic polymer which can lead to low cell affinity and inflammatory effect towards host tissue or organ. For that reason, many researchers have incorporated PVDF with hydrophilic fillers such as polyurethane (PU), trifluoroethylenen (TrFE), chitosan, graphene oxide (GO), and polyhedral oligomeric silsesquioxane-epigallocatechin gallate (POSS-EGCG) conjugate to increase its water absorption ability and specific cell recognition sites without losing its mechanical integrity [8-11].

Polyvinyl alcohol (PVA) is a semi-crystalline hydrophilic polymer, which is widely used in biomedical applications due to its biocompatibility to most types of tissue, ability to absorb protein molecules, ability to adopt a minimum cell adhesion, and highly stable at wide range of temperature [12-13]. Other than that, the crystalline structure consists of the hydroxyl group, which allows high degree of miscibility with other materials and will act as a cell-bind recognition site at the scaffold during the regeneration process [14]. Therefore, PVA can be blended with PVDF to obtain a scaffold with desired physical properties that are suitable for cell and tissue regeneration processes.

In this study, the physical properties of electrospun PVDF/PVA was investigated using tensile strength, water contact angle (WCA), swelling test, morphological characterisation, electrical characterisation, Fourier transform infrared (FTIR) spectroscopy and in-vitro cytotoxicity testing. To date, no studies on the fabrication of single phase PVDF/PVA nanofibre scaffold using the electrospinning technique are reported.

2. MATERIAL AND METHODS

2.1 Preparation of Electrospun PVDF/PVA

The PVDF ($\approx 534,000$ g/mol, Sigma) and PVA ($\approx 89,000$ g/mol, Sigma) were dissolved in 5 mL DMSO (≈ 84.17 g/mol, Merck) solution forming 0.15% (w/v) concentration with varied PVDF-to-PVA ratio as prepared in Table 1. The electrospinning apparatus was set up horizontally as illustrated in Figure 1. The 5-mL polymer solution was placed in a 5-mL plastic syringe with 23G needle size and an injection rate of 1.0 mL/h. The needle tip of the syringe was connected to a 5-kV voltage power with the tip-to-collector distance of 13 cm.

Table 1 PVDF-to-PVA ratio used in fabrication process

PVDF-to-PVA ratio	Type of sample
100:0	100PVDF/0PVA or Neat PVDF
95:5	95PVDF/5PVA
90:10	90PVDF/10PVA
85:15	85PVDF/15PVA
80:20	80PVDF/20PVA
75:25	75PVDF/25PVA

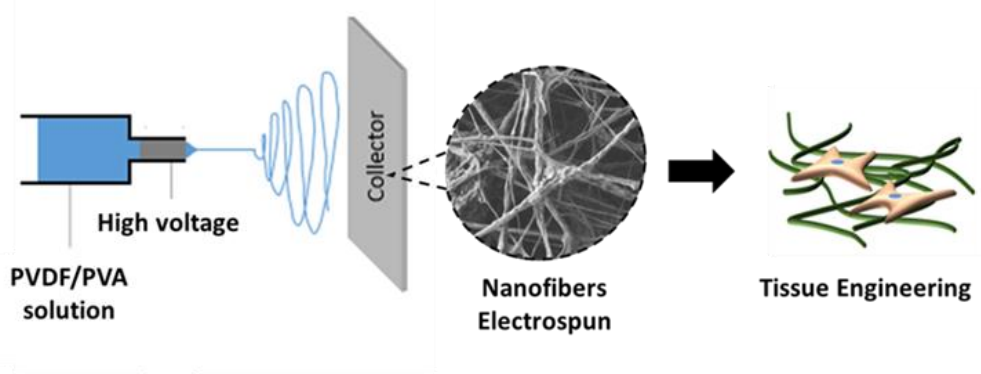


Figure 1. Illustration of electrospinning process and its application.

2.2 Characterization of PVDF/PVA Electrospun

The tensile test was conducted to obtain the stress-strain graph by using a universal tester according to ASTM D-882 (Instron, 2018) at a strain rate of 10 mm/min and load strength of 5 kN at room temperature until failure. Then, the surface morphological properties of nanofibre were observed using Field emission scanning electron microscope (FESEM model JSM-7800F, JEOL) with 100×–10000× magnification. From the magnified image, the diameter of nanofibre was determined using ImageJ software to analyze at least 100 different fibres. The hydrophilicity was assessed using water contact angle (WCA) by recording sample surface image of 1µL of deionized water using the video contact angle system (VCA Optima, Ast Products Inc) and calculated the swelling percentage of sample in 10 mL of PBS for 5 days using Equation 1. The electrical property was evaluated by measuring conductivity level of PVDF/PVA nanofibre using a multimeter (SANWA, Japan), where the resistance value taken was used to calculate the conductivity using Equation 2. Lastly, the structural and interaction characteristic was determined using the Fourier transform infrared spectroscopy (FTIR, Perkin Elmer Frontie) at wavelength from 400 to 4000 cm⁻¹.

$$\text{Degree of Swelling (\%)} = \frac{w_f - w_i}{w_f} \times 100 \quad (1)$$

Where, w_f represents the weight of swollen nanofibre at a predetermined time and w_i is the initial weight of the nanofibre.

$$\text{Conductivity} = \frac{1}{\rho} = \frac{l}{RA} \quad (2)$$

Where, ρ represents the electrical resistivity through a specific area, R is the resistance given by the sample, l signifies the sample thickness used, and A is the surface area of sample.

2.2 Cytotoxicity Analysis using Human Dermal Fibroblast (HDF) Cell

In this experiment, the 5th to 10th passages of HDF cells were used and cultured in T-flasks comprising DMEM medium supplemented with 10% (v/v) fetal bovine serum (FBS), 1% (v/v) L-glutamine, and 1% (v/v) penicillin/streptomycin. The cells were incubated at 37 °C with 5% CO₂ and the medium was refreshed every 3 days. The nanofibrous samples were seeded with HDF cell suspension at 1×10^4 cells/ml in 24-well culture plates. The cells were allowed to attach for at least 10 min and the medium was refreshed with a new culture medium before the samples were subjected to incubation periods depending on assay requirements [15]. MTT assay was performed to test cell proliferation and metabolic activity by quantifying absorbance of purple formazan crystals reflecting the volume of the survived cell after 24 and 48 hours of incubation. Nanofibrous samples were moved to new wells, applying the MTT reagent to each well. Then the samples were incubated for 4 hours before forming crystals. Solution absorbance was measured at 570 nm using a microplate reader. The cells also were stained using Live/Dead kit assay containing polyanionic dye calcein (green-live cell) and ethidium homodimer-1, EthD-1 (red-dead cell). The photomicrograph of the live-dead cell was analysed under fluorescence microscope (Carl Zeis Axio Vert A1).

3. RESULTS AND DISCUSSION

3.1 Mechanical Characterisation

Mechanical properties play a significant role as a crucial element in tissue engineering especially during surgeries. An ideal electrospun nanofibre should be durable, flexible, and able to sustain high pressure when tissue begins to infiltrate the scaffold, and increased growth [18]. The tensile properties of the tested samples are summarised in Table 2. The tensile strength and Young's modulus of the neat electrospun PVDF was 1.33 ± 0.7 and 9.61 ± 0.2 MPa, respectively. The alteration of PVDF-to-PVA ratio from 5% to 10% increased the tensile strength and Young's modulus significantly. However, the higher inclusion of PVA (15% to 25%) drastically reduced the mechanical integrity of the electrospun nanofibre. This reduction may be caused by the loss of PVDF phases in the formulation as shown in the SEM micrograph. The higher reduction of PVDF ratio produced unstable electrospinning process which leads to the high number of beads that affects the structural integrity of the electrospun fibres performance. Besides, study also reported that the mechanical strength will increase when the diameter of nanofiber decreases [8]. Sample 90PVDF/10PVA showed smaller average diameter has an optimal tensile strength of 1.72 ± 0.6 MPa and Young' modulus of 22.03 ± 0.5 MPa. Previous study reported that the tensile strength for natural soft collagenous tissues include cartilage, cornea, nerve, and skin is around 1 to 10 MPa [3,16]. Therefore, based on these findings it can be said that the modified electrospun nanofibre meets the requirement as a potential tissue scaffold.

Table 2 The tensile strength, Young's modulus and average diameter nanofibre of neat PVDF and electrospun PVDF/PVA

PVDF/PVA sample	Tensile strength (MPa)	Young Modulus (MPa)	Average Diameter (nm)
100PVDF/0PVA	1.33 ± 0.7	9.61 ± 0.2	210
95PVDF/5PVA	1.76 ± 0.1	10.86 ± 0.3	185
90PVDF/10PVA	1.72 ± 0.6	22.03 ± 0.5	161
85PVDF/15PVA	0.96 ± 0.2	7.09 ± 0.1	194
80PVDF/20PVA	0.76 ± 0.3	6.14 ± 0.3	281
75PVDF/25PVA	0.58 ± 0.3	4.78 ± 0.1	353

3.2 Morphology Characterisation

Figure 2 displays the pure PVDF and PVDF / PVA fibrous nanostructure fibres with their diameter distribution. Figure 2(a)–1(c) indicates the nanofibre diameter decreased from 210 to 161 nm as the PVA ratio approached 10% (w / v) of PVDF polymer solution. The limited volume of PVA incorporation has dramatically changed the viscosity of the PVDF polymer solution, resulting in improved dispersion due to adequate jet stretching time and solvent volatilisation. Significant morphological changes were observed as the PVA ratio increased from 15% in 85PVDF/15PVA to 25% in 75PVDF/25PVA. Further ratio modification can cause more bead-on-string formation resulting in greater pore size and lower porosity percentage. The probable explanation behind the non-homogenous surfaces is due to the reduction of dielectric potential due to the low viscosity of the conductive PVDF polymer solution that developed an unstable polymer projection during the electrospinning phase. In tissue engineering applications, electrospun 's diameter size can significantly affect the fibrous surface area and cell attachment volume, which smaller diameter will provide high density for cell cultivation [16-17]. This advantage would much support cells or tissues with minimal endogenous regeneration ability or replacement of damaged cells such as the brain and nervous system.

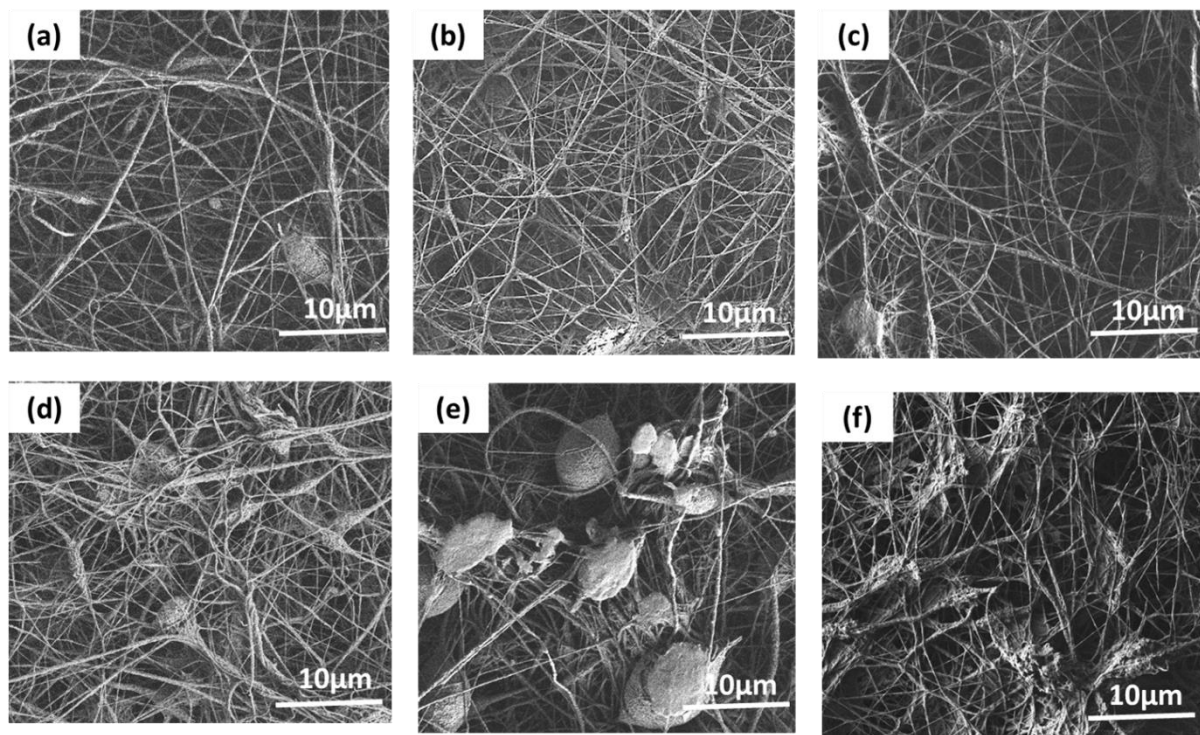


Figure 2. FESEM micrograph of electrospun sample at PVDF to PVA ratio (a) 100:0, (b) 95:5, (c) 90:10, (d) 85:15, (e) 80:20, and (f) 75:25.

3.3 Water Contact Angle (WCA)

In the field of tissue engineering, the tissue scaffold surface is the first part to contact the biological structure that enables the desired effects of tissue growth to be biocompatible. WCA is one of the wettability methods used to study the surface efficiency of the sample [19-20]. Figure 3 displays the WCA and the images of water on the samples of electrospun. The electrospun 100PVDF/0PVA exhibited a superhydrophobic surface at WCA value of 130.50°, this may occur due to its low surface energy and hydrophobic properties. Nevertheless, adding PVA monomer in PVDF formulation have significantly reduced the WCA to lesser than 90°, which indicated the hydrophilic surface content. In the PVDF/PVA electrospun surface, the introduction of hydroxyl and carbonyl groups from PVA monomer leads to modification of the polarity of the surfaces by

increasing their specific hydrogen bond and the electrostatic forces with the water molecules. Figure 3(d)–(f) shows that the higher PVA addition increases the WCA value marginally as a result of a rise of bead string formation resulting in a rugged surface with 5%, 10% ratio compared to PVA, as demonstrated by the FESEM micrograph in Figure 2 (d)–(f). In general, increased surface roughness leads to a low water drop-material contact area that interrupts the interface of water and fibre, which further decreases the contact area between artificial and biological specimens. In consequence, low WCA would also be beneficial for the tissue engineering application as it will optimise performance when the scaffold is assigned to the wound site of the tissue [19,21].

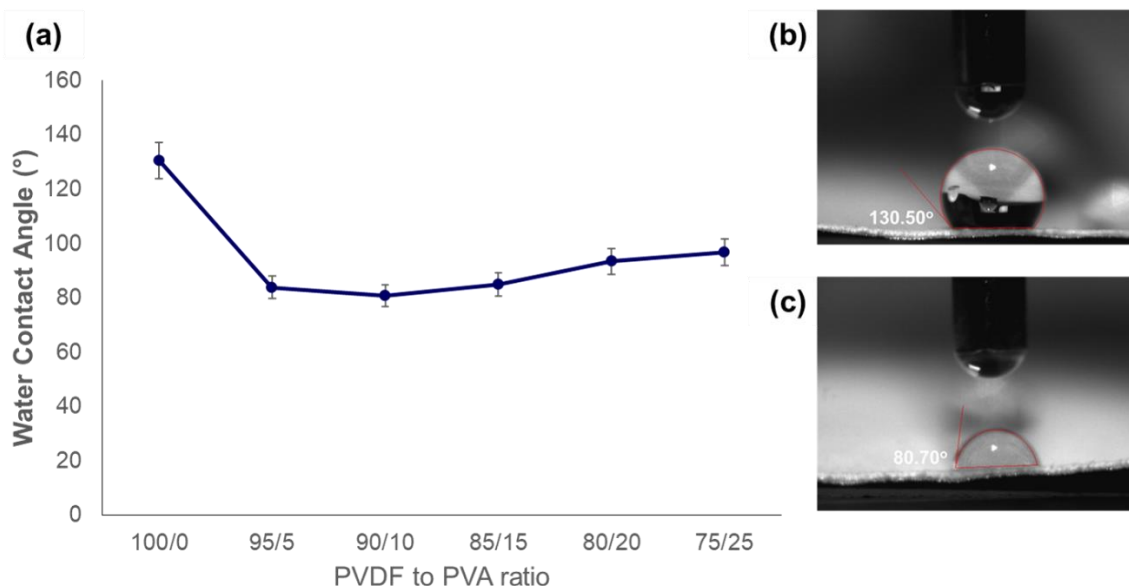


Figure 3. (a) Surface contact angle of electrospun PVDF/PVA samples and WCA image of (b) 100PVDF/0PVA and (c) 90PVDF/10PVA.

3.4 Degree of Swelling

The ability of the sample to absorb water molecules plays a major role during cell growth, especially during cell seeding. It will also influence the potential of the electrospun composite to maintain its shape during the application. Figure 4 presents the degree of swelling percentage of the neat PVDF and its modification containing electrospun PVA. The results reveal that the inclusion of PVA strongly influences the swelling capacity of the electrospun nanofibre and increased it from $4.76 \pm 1.3\%$ (for 100PVDF/0PVA) to $69.84 \pm 1.5\%$ (for 90PVDF/10PVA) after 24 hr of immersion. The increased swelling percentage could be attributed to the fine inter- and intra-polymer reactions and the addition of hydrophilic groups in the electrospun PVDF/PVA. This observation is in corroborates with the WCA experiment, which the presence of PVA increased the specific interaction between the electrospun surfaces as a substrate to water molecule through the hydrogen bond. The increases can also be observed after 24 hr of immersion, which indicate a good signal in maintaining the swelling behaviour throughout the healing process because it will affect the diffusion process of signaling molecules and nutrients [22].

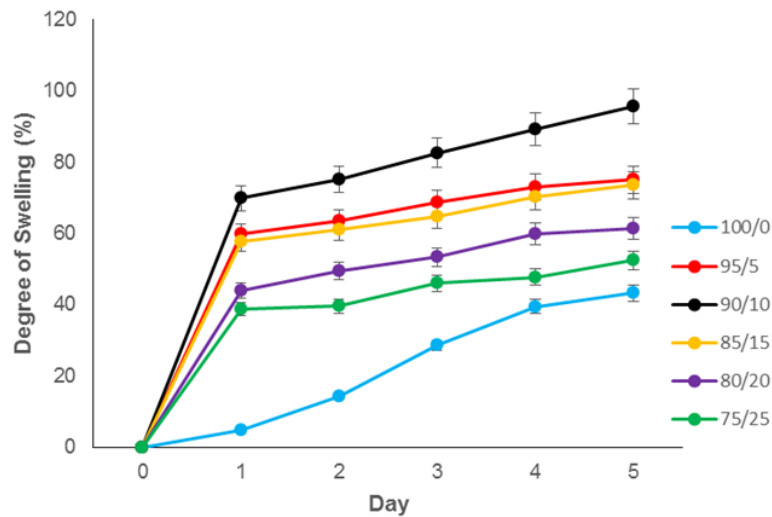


Figure 4. Time-dependent degree of swelling for neat PVDF and electrospun PVDF/PVA.

3.5 Conductivity Analysis

The conductivity of each sample was calculated using Equation 2 and is presented in Table 3. The conductivity of the neat PVDF nanofibre was 4.023×10^{-4} S/cm. The conductivity of electrospun PVDF was contributed by the formation of β -phase that plays an important role in piezoelectric and pyroelectric performance [23-24]. The conductivity increased with increasing amount of PVA until 10% inclusion at 5.991×10^{-4} S/cm. This might be due to the electrospinning process causing the dielectric polarisation of the dielectric PVA monomer. It has led to the increase in intermolecular distance and the mobility of the chains, which accelerates the orientation of the modified polymer molecules into more crystalline structure. Besides, this improvement also contributed by the uniform dispersion and proper interaction of PVDF and PVA forming a uniform, porous, and well fibre structure, which will act as a charge carrier (hole) motion for the conducting electrical charges [25]. However, higher inclusion has reduced the conductivity due to the higher loss of PVDF monomer and increased bed-string fibre which causing low electrical motion carrier throughout the electrospun samples.

Table 3 The conductivity level for different PVDF to PVA ratio

PVDF/PVA Ratio	Conductivity (S/cm)
100/0	4.023×10^{-4}
95/5	4.834×10^{-4}
90/10	5.991×10^{-4}
85/15	4.917×10^{-4}
80/20	4.123×10^{-4}
75/25	3.533×10^{-4}

In general, the bioactive conductive scaffolds give huge advantages during cell attachment and proliferation where it will improve intracellular electrical signaling sensitive cells increase cytoplasmic content, especially for fibroblasts, neurons, myoblasts, and osteoblasts cell type [26]. Study reported that scaffolds with conductivity from 1.21 to 4.54×10^{-4} S/cm demonstrate excellent work in enhancing myoblasts proliferation, while scaffolds conductivity around 3.5×10^{-3} S/cm show good growth activities on cardiomyocyte and neuron cells [27]. A previous study also reported that the scaffolds with conductivity from 6.5×10^{-4} to 1.4×10^{-3} S/cm show good adhesion and proliferation of cells using rabbit adipose-derived mesenchymal stem cells [28]. Accordingly, the electrospun PVDF/PVA prepared in this study might be suitable for electrical sensitive tissue applications. Among the formulations, 90PVDF/10PVA is considered as

a proper condition for further testing due to its good morphology, mechanical, and wettability properties.

3.6 FTIR Analysis

The chemical composition of PVDF, PVA, and PVDF-PVA blended ratio 90:10 nanofibre were characterised using FTIR spectrum. Figure 5 (a) shows a strong peak at 1400 cm^{-1} that corresponds to the C-H antisymmetric deformation represents a typical PVDF nanofibre characteristics. Meanwhile, strong peaks at 1072 , 1174 , and 1275 cm^{-1} correspond to the vibrational of C-F bond that was found in the PVDF nanofibre [29]. Figure 5 (b) shows the spectrum for PVA film. The characteristics band at peaks 3398 and 3430 cm^{-1} indicate the interconnection between the hydrogen bond of hydroxyl functional group (O-H) [30-31]. The interaction between PVDF and PVA is depicted in Figure 5 (c), which shows the interconnection between the two materials that can be observed through the new peak at 3363 cm^{-1} that indicates the association of PVDF to the hydroxyl group of PVA [30]. New peak at 2850 cm^{-1} was found in PVDF/PVA transmission profile which donates from the C-H bond. Other strong peaks at 1071 , 1275 , and 1400 cm^{-1} were found in PVDF/PVA spectrum indicate the possible stretching vibration of C-F from PVDF and C-O-C bond from PVDF/PVA [10,12,29]. Meanwhile, the vibration band occurring at 839 and 831 cm^{-1} indicate CF_2 bending and CF_2 rocking corresponding to the α and β phase [12,31].

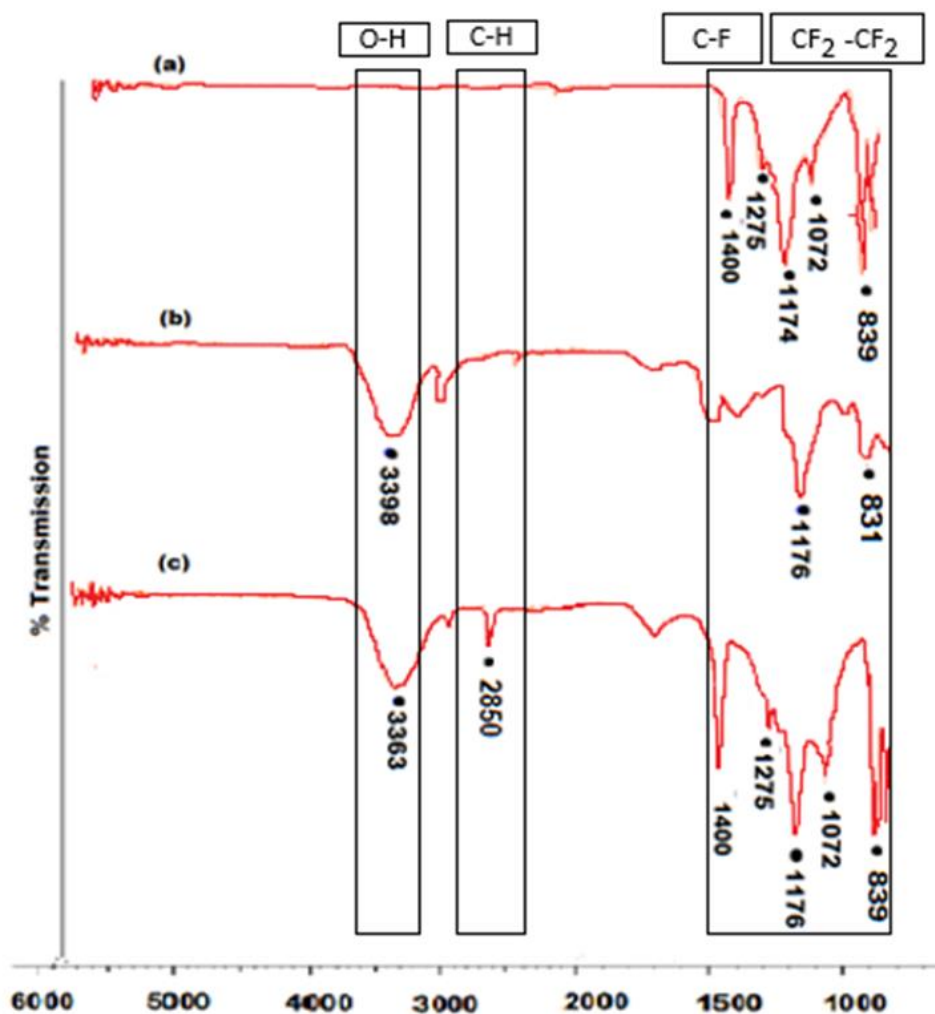


Figure 5. FTIR spectra of electrospun (a)PVDF, (b)PVA and (c)PVDF/PVA nanofibre.

3.7 In-vitro Cytotoxicity

MTT assay was conducted to investigate the cytotoxicity potential of neat PVDF and electrospun PVDF / PVA using HDF cells. The standard 2D culture was used as the negative control, while the positive control was assed by adding Trixton-X. Figure 6 (a) shows that the proliferation of cells on the electrospun PVDF/PVA was higher than that of the neat electrospun PVDF, indicating that the composite polymer might have enhanced the adhesion and differentiation of HDF cells. Besides, the PVA inclusion in electrospun PVDF/PVA show better attachment and proliferative behaviour of cells after 24 hr of seeding process compared to neat electrospun PVDF as presented in Figure 6 (b) and (c). The live HDF cells (green colour) displayed the complete stretching morphology for both scaffolds. However, the cells are well spreading and interaction onto electrospun PVDF/PVA surfaces compared to the neat electrospun PVDF as shown in fluorescence image. The addition of PVA have altered the wettability and introduced biochemical signals onto the electrospun surface which make it favourable for specific cells–substrate interaction [32]. Furthermore, the ability of the electrospun PVDF/PVA to absorb fluid acts as an important reason for the proliferative performance of HDF cells, because it aids in transferring metabolic products and nutrients efficiently during the cell culture.

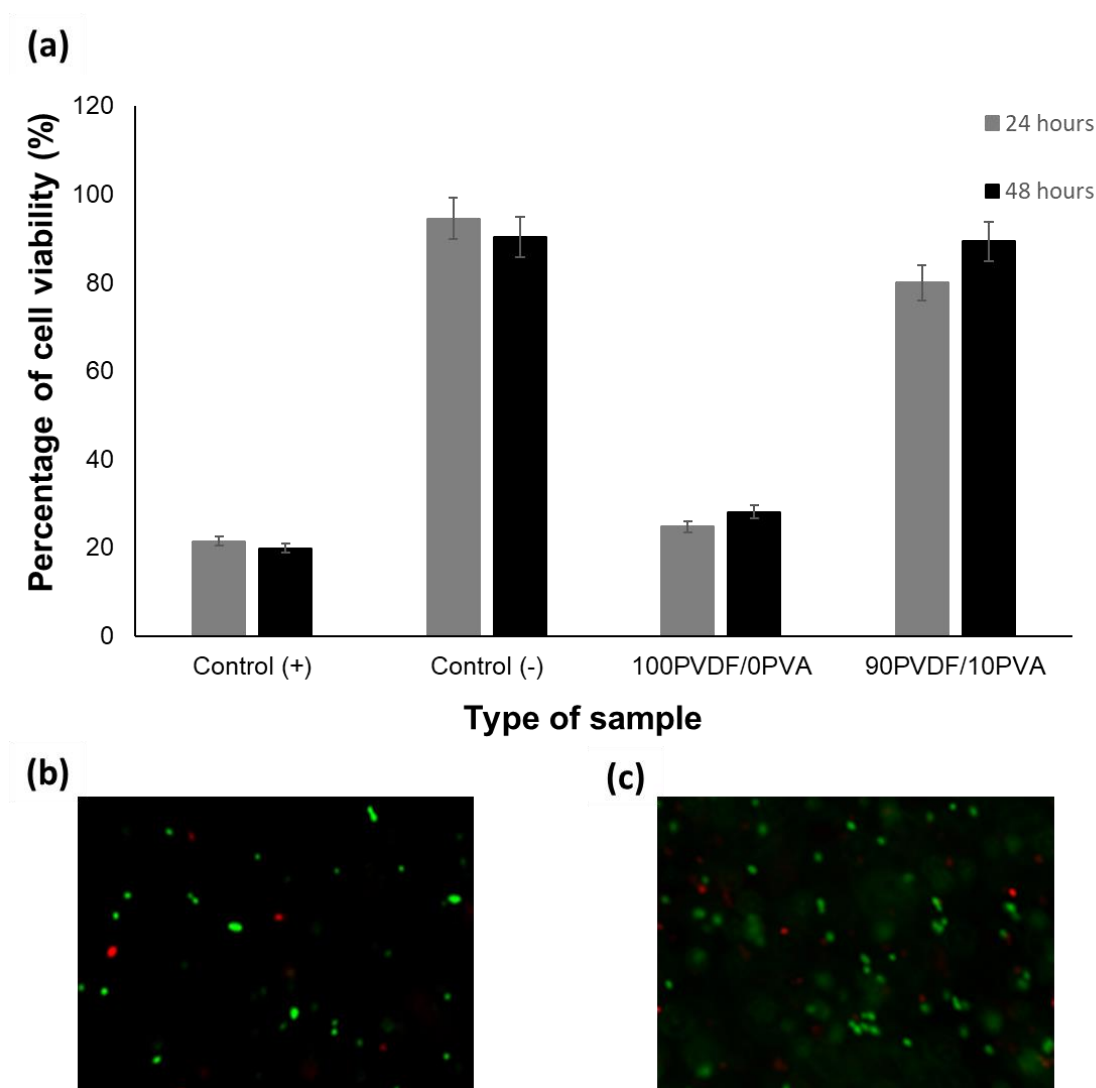


Figure 7. (a)Percentage viability of HDF cells using MTT assay; fluorescence micrograph of HDF cells after 24 hr onto electrospun (b) 100PVDF/PVA and (c) 90PVDF/10PVA.

4. CONCLUSION

Herein, PVDF/PVA nanofibrous membrane scaffolds were produced by electrospinning at optimised condition with average fibre diameter ranged from 160 to 180 nm. Smooth surface of fibres morphology was found for the optimal electrospun nanofibre with excellent mechanical, wettability, and electrical properties at PVDF-to-PVA ratio of 90:10 (90PVDF/10PVA). The FTIR spectra confirmed the good interaction between the PVDF chain and PVA monomer as supported by other testings. The PVDF/PVA has good biocompatibility and nontoxic towards HDF cells, where the modified nanofibrous scaffold have successfully supported the cell differentiation and proliferation process. Considering the overall results, the 90PVDF/10PVA ratio composition has a good potential as potential artificial soft tissue scaffold materials and future works need to be conducted to reassure the effect of the nanofibrous membrane for specific targeted tissue engineering applications.

ACKNOWLEDGEMENTS

This work is supported by the Ministry of Higher Education Malaysia through the Malaysia Technical University Network Grant Scheme (MTUN- Vote number K124, K243) and Fundamental Research Grant Scheme FRGS/1/2019/TK10/UTHM/03/1 (FRGS-K220), as well as Universiti Tun Hussein Onn Malaysia (UTHM) through the Geran Penyelidikan Pascasiswazah (GPPS-Vot number H458).

REFERENCES

- [1] Okutan, N., Terzi, P., and Altay, F., *Food Hydrocoll*, **39** (2014) 19-26.
- [2] Meng, Z. X., Xu, X. X., Zheng, W., Zhou, H. M., Li, L., Zheng, Y. F., & Lou, X., *Colloids Surf B Biointerfaces*, **84**, 1 (2011) 97-102.
- [3] Khoo, W., Koh, C. T., & Lim, S. C., *J Mech Eng*, **4** (2017) 223-233.
- [4] Franco, R. A., Nguyen, T. H., & Lee, B. T., *J Mater Sci Mater Med*, **22**, 10 (2011) 2207.
- [5] Hackett, J. M., Dang, T. T., Tsai, E. C., & Cao, X., *Mater*, **3**, 6 (2010) 3714-3728.
- [6] Shao, H. J., F., Wang, H., & Lin, T., *Adv*, **5**, 19 (2015) 14345-50.
- [7] Ribeiro, C., Correia, D. M., Ribeiro, S., Sencadas, V., Botelho, G., & Lanceros-Méndez, S., *Eng Life Sci*, **15**, 4 (2015) 351-356.
- [8] Jeong, H. G., Han, Y. S., Jung, K. H., & Kim, Y. J., *Nanomater*, **9**, 2 (2019) 184.
- [9] Hamzah, M. S. A., Azize, A. H. A., Yusof, S., Noor, S. M., & Nayan, N. H. M., "Electrospinning and controlled release studies of polyvinylidene fluoride/pectin electrospun loaded with crocin as neuroprotective membrane prospect," in *Proceedings of National Innovation & Invention Competition 2019*, Johor, Malaysia: Universiti Tun Hussein Onn Malaysia, (2019) 335-338
- [10] Park, J. A., Cho, K. Y., Han, C. H., Nam, A., Kim, J. H., Lee, S. H., & Choi, J. W., *Sci Rep*, **9**, 1 (2019) 383.
- [11] Moradi, R., Karimi-Sabet, J., Shariaty-Niassar, M., & Koochaki, M., *Polym*, **7**, 8 (2015) 1444-1463.
- [12] Nkhwa, S., Lauriaga, K. F., Kemal, E., & Deb, S., "Poly (vinyl alcohol): physical approaches to designing biomaterials for biomedical applications," In *Conference Papers in Science*, Hindawi, (2014).
- [13] Uslu, I., Daştan, H., Altaş, A., Yayli, A., Atakol, O., & Aksu, M. L., *e-Polym*, **7**, 1 (2007).
- [14] Teodorescu, M., Bercea, M., & Morariu, S., *Biotechnol Adv*, **37**, 1 (2019) 109-131.
- [15] Hamzah, M. S. A., Razak, S. I. A., Kadir, M. R. A., Bohari, S. P. M., & Nayan, N. H. M., *J Polym Eng*, **40**, 5 (2020) 421-431.
- [16] Hamzah, M. S. A., Austad, A., Razak, S. I. A., & Nayan, N. H. M., *Int J Struct Integr*, **10**, 5 (2019) 704-713.
- [17] Pezeshki-Modaress, M., Zandi, M., & Rajabi, S., *Prog Biomater*, **7**, 3 (2018) 207-218.

- [18] Alhasssan, Z. A., Burezq, Y. S., Nair, R., & Shehata, N., *J Nanomater*, (2018) 1-12.
- [19] Saudi, A., Rafienia, M., Zargar Kharazi, A., Salehi, H., Zarrabi, A., & Karevan, M., *Polym Adv Technol*, **30**, 6 (2019) 1427-1440.
- [20] Raffaini, G., & Ganazzoli, F., *Macromol Biosci*, **7**, 5 (2007) 552-566.
- [21] Menzies, K. L., & Jones, L., *Optom Vis Sci*, **87**, 6 (2010) 387-399.
- [22] Pan, J. F., Liu, N. H., Sun, H., & Xu, F., *PLoS One*, **9**, 11 (2014).
- [23] Rianjanu, A., Winardianto, B., Munir, M., Kartini, I., & Triyana, K., *Int J Adv Sci Eng Inf Technol*, **6**, 5 (2016) 675-681.
- [24] Aqeel, S. M., Wang, Z., Than, L., Sreenivasulu, G., & Zeng, X., *RSC Adv*, **5**, 93 (2015) 76383-76391.
- [25] Shahini, A., Yazdimamaghani, M., Walker, K. J., Eastman, M. A., Hatami-Marbini, H., Smith, B. J., Ricci, J.L., Madihally, S.V., Vashae, D., & Tayebi, L., *Int J Nanomed*, **9** (2014) 167.
- [26] Balint, R., Cassidy, N. J., & Cartmell, S. H., *Acta Biomater*, **10**, 6 (2014) 2341-2353.
- [27] Zhao, Y. H., Niu, C. M., Shi, J. Q., Wang, Y. Y., Yang, Y. M., & Wang, H. B., *Neural Regen Res*, **13**, 8 (2018) 1455.
- [28] Dong, R., Zhao, X., Guo, B., & Ma, P. X., *ACS Appl Mater Interfaces*, **8**, 27 (2016) 17138-17150.
- [29] Park, M. J., Gonzales, R. R., Abdel-Wahab, A., Phuntsho, S., & Shon, H. K., *Desalination*, **426** (2018) 50-59.
- [30] Boccaccio, T., Bottino, A., Capannelli, G., & Piaggio, P., *J Membr Sci*, **210**, 2 (2002) 315-329.
- [31] Martins, P., Lopes, A. C., & Lanceros-Mendez, S., *Prog Polym Sci*, **39**, 4 (2014) 683-706.
- [32] Ghasemi-Mobarakeh, L., Prabhakaran, M. P., Morshed, M., Nasr-Esfahani, M. H., & Ramakrishna, S., *Biomater*, **29**, 34 (2008) 4532-4539.

